Radial dependence of TiO_2 nanoparticles synthesised in jet-wall stagnation flames

Eric J Bringley, Manoel Y Manuputty, Casper Lindberg, Gustavo Leon, Jethro Akroyd, Markus Kraft

June 25th, 2021

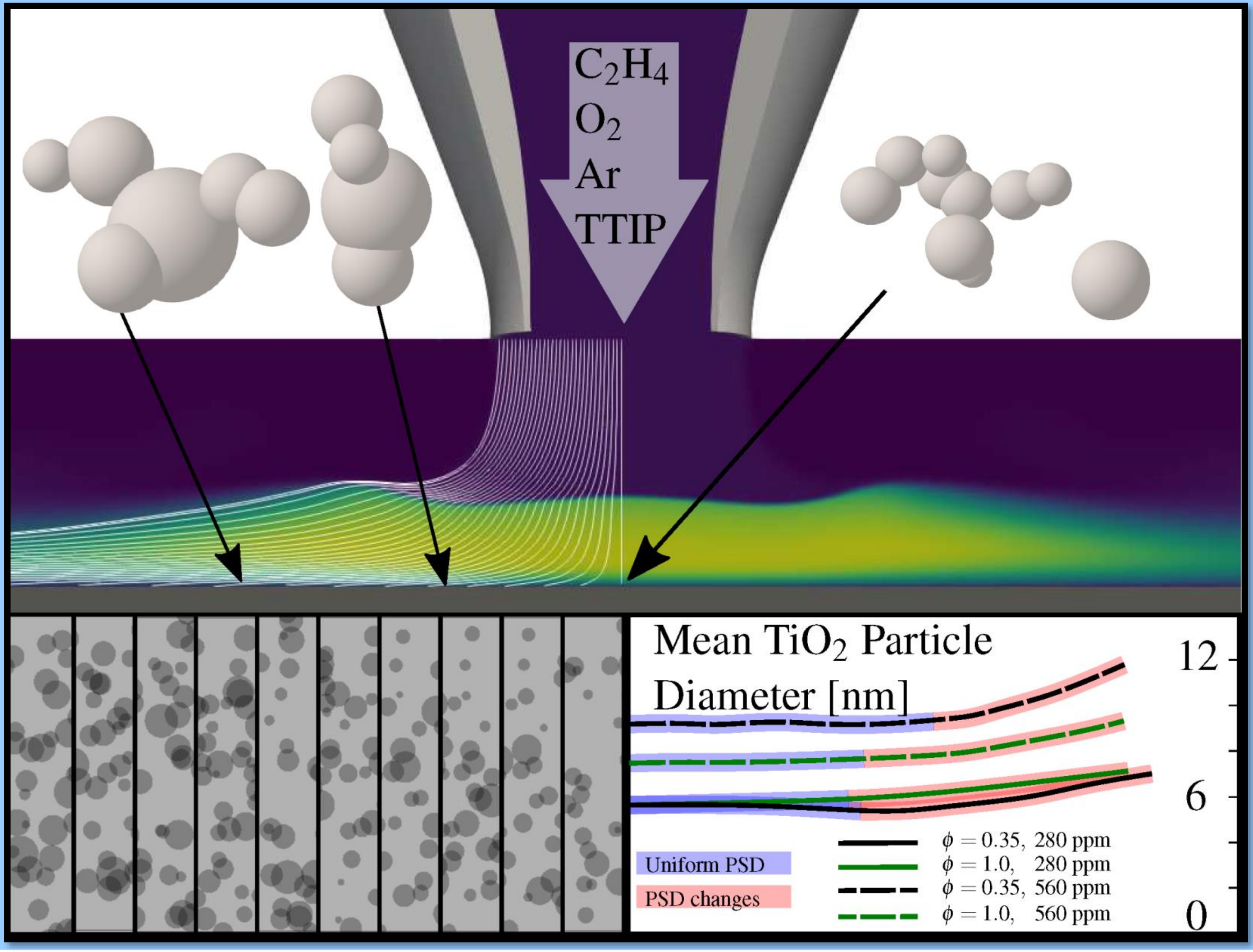

Cambridge Particle Meeting,
Cambridge, UK

Titania (TiO_2)

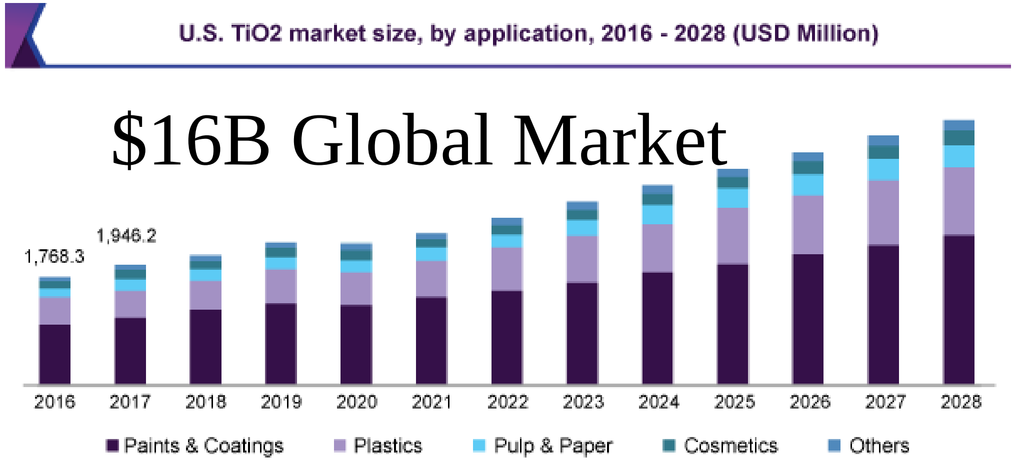

$16B Global Market

Source: www.grandviewresearch.com

Stable Phases (Anatase, Rutile)

Metastable Phases (TiO_2-II)

[1]

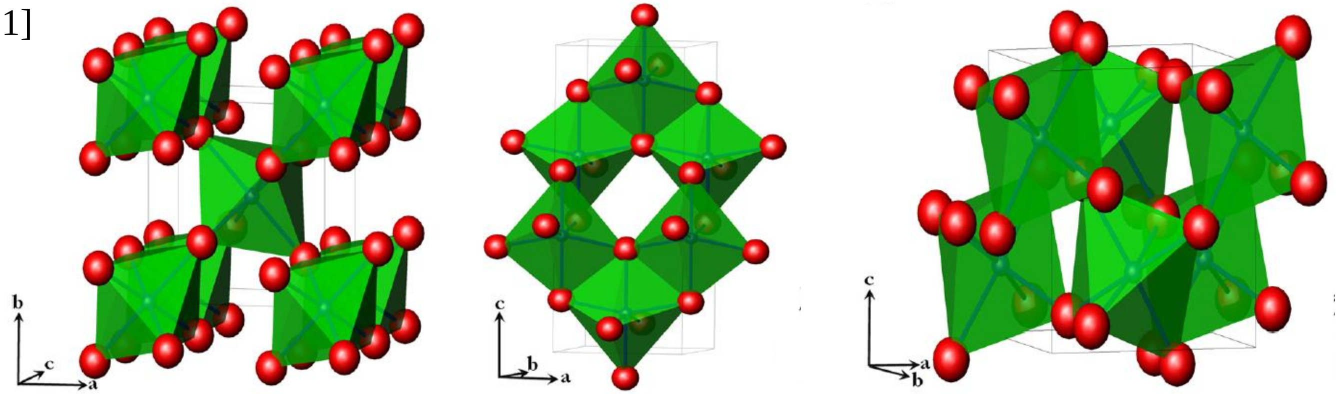

[2]

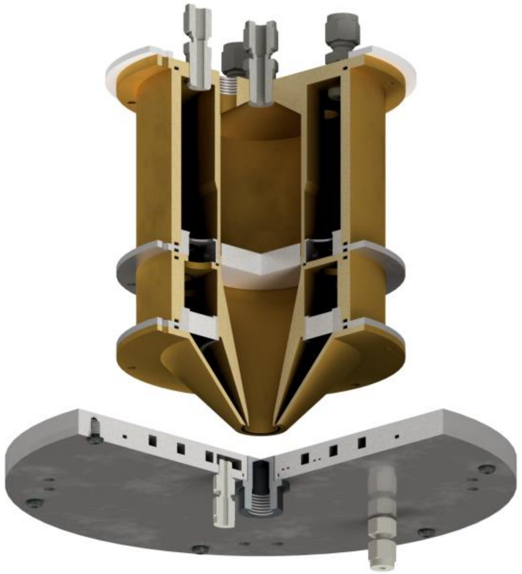

[1] Aravindan et. al (2015) doi: 10.1016/j.mattod.2015.02.015
[2] Wu et. al (2020) doi: 10.1002/smtd.202000928

Jet-wall stagnation flames for TiO_2 synthesis

Short residence times produce small particles

Do the deposited particles change as a function of the radius? If so, where?

≈ 1 – 1.5 nozzle radius

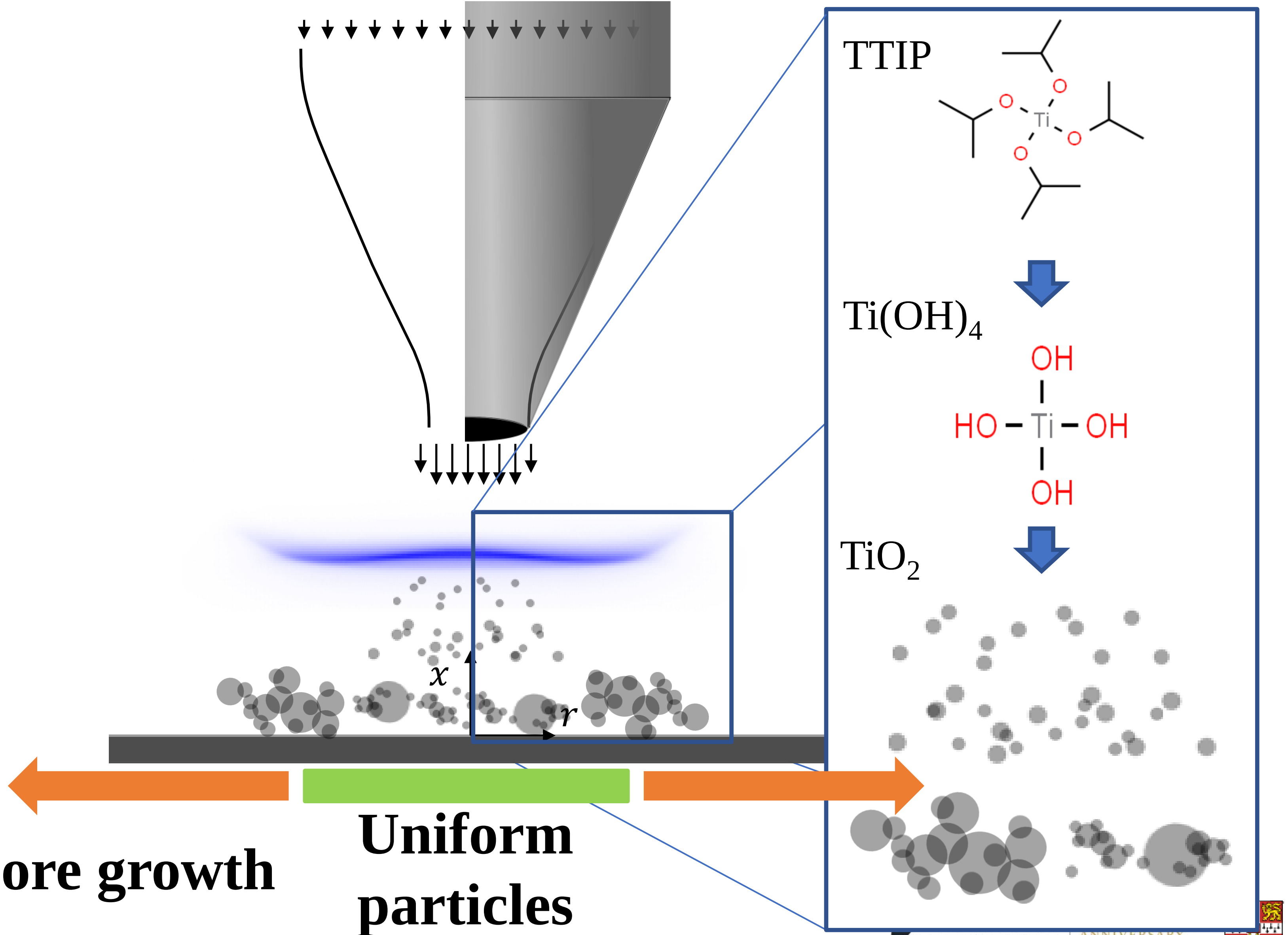

more growth

Uniform particles

Simulations

Equivalence ratios
$\phi = 1.0$ and 0.35

TTIP loadings
280 and 560 ppm

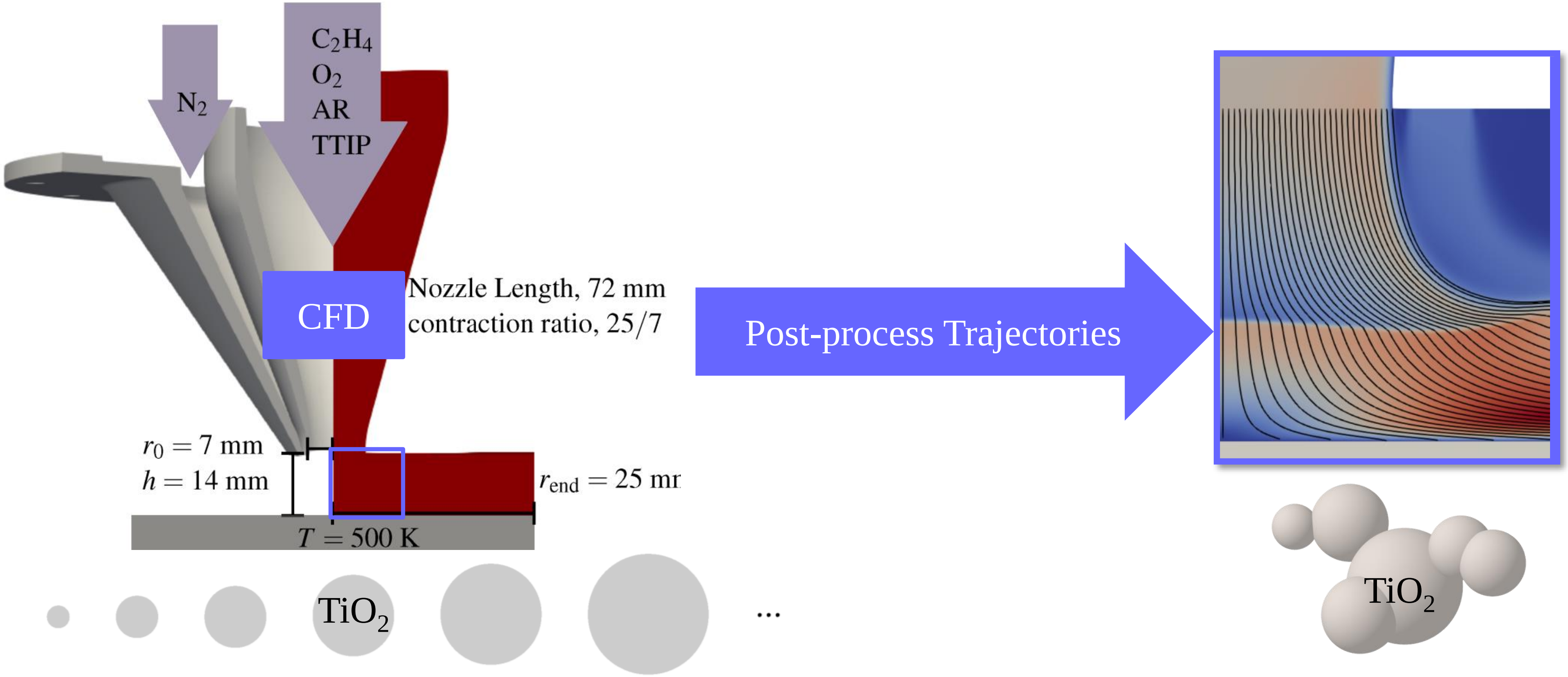

Flame centreline data

Two equivalence ratios produce different $Ti(OH)_4$ profiles

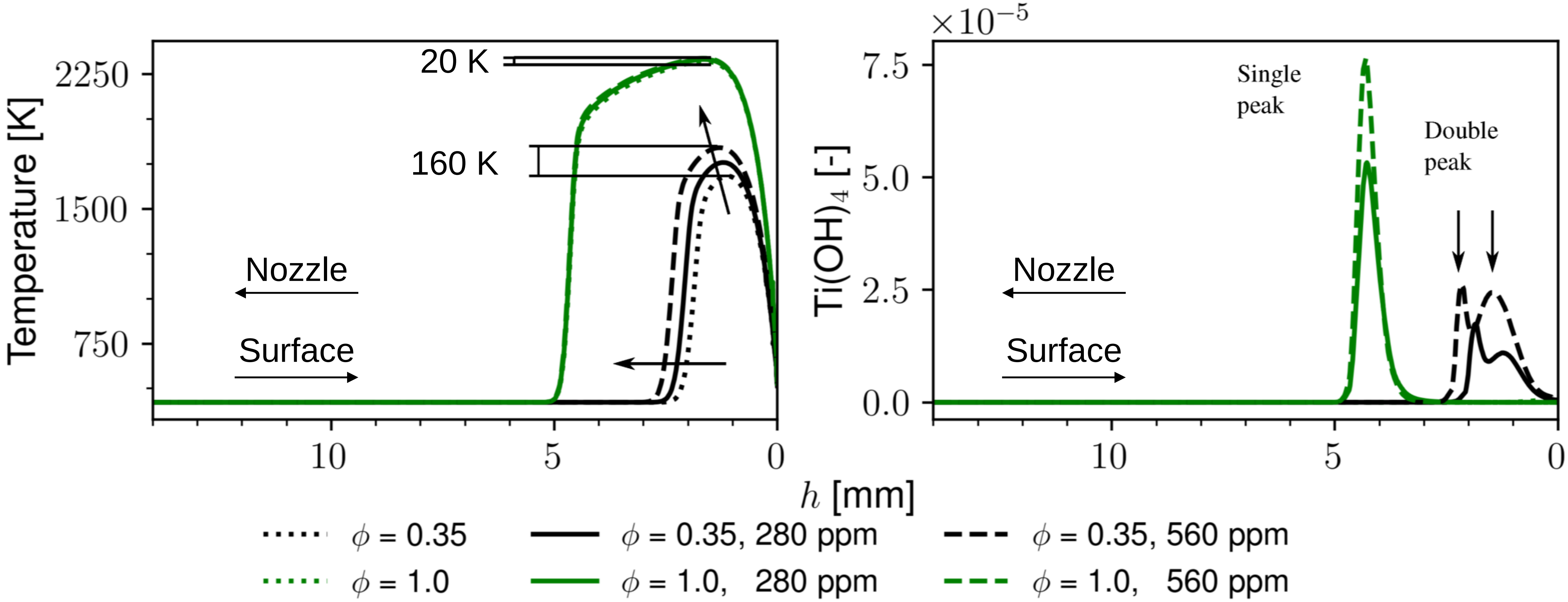

Lagrangian trajectories

As trajectories travel further, the residence time increases.

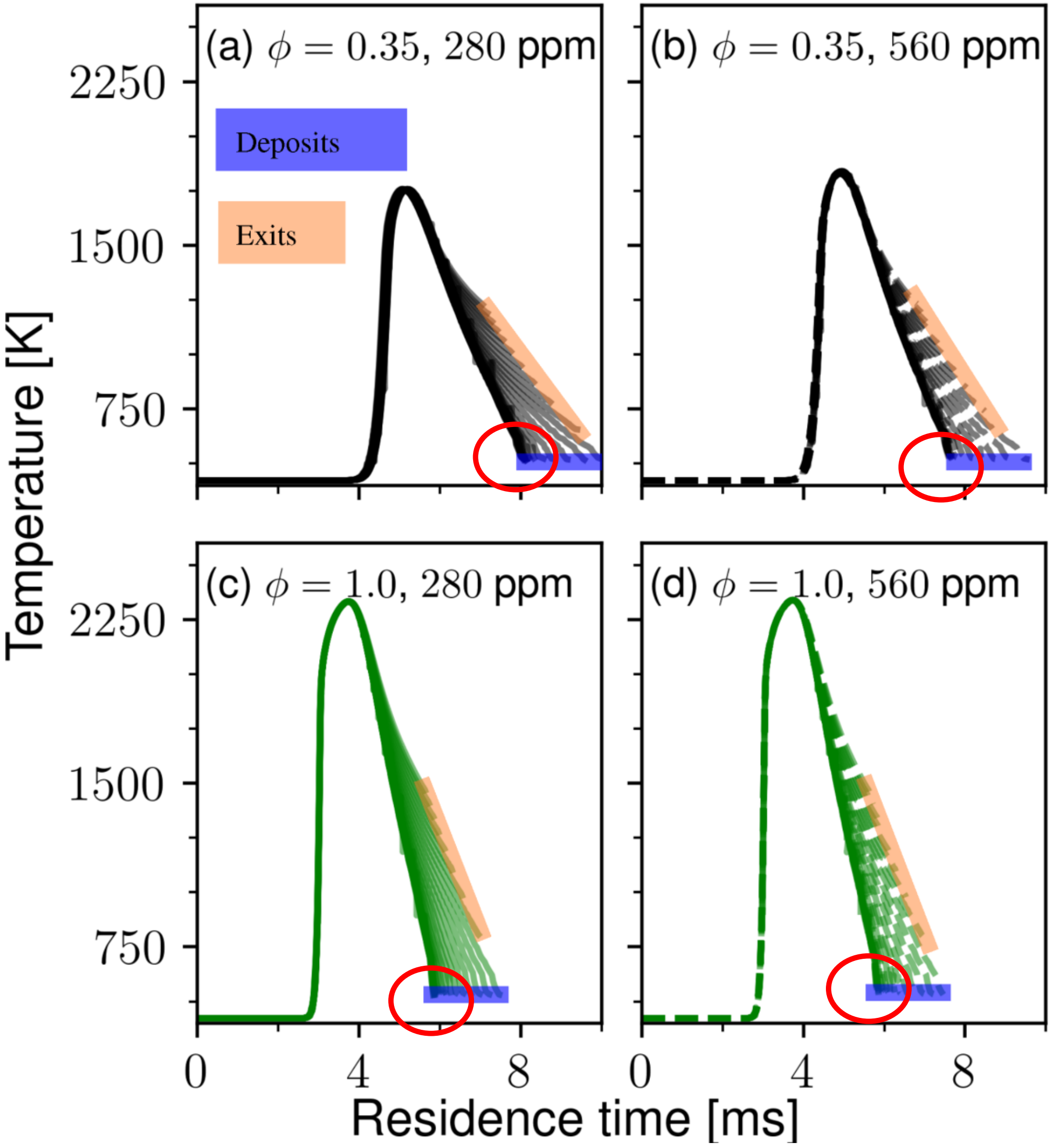

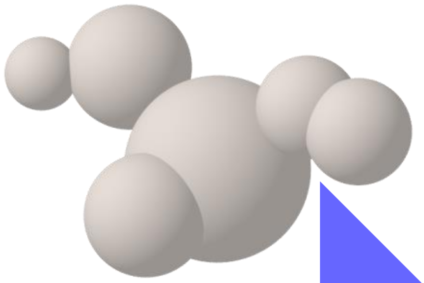

Post-processed with Detailed Particle Model

Aggregate and primary size distributions

As trajectories move radially outwards,
the aggregates grow bigger, but primaries remain similar in size

Aggregates

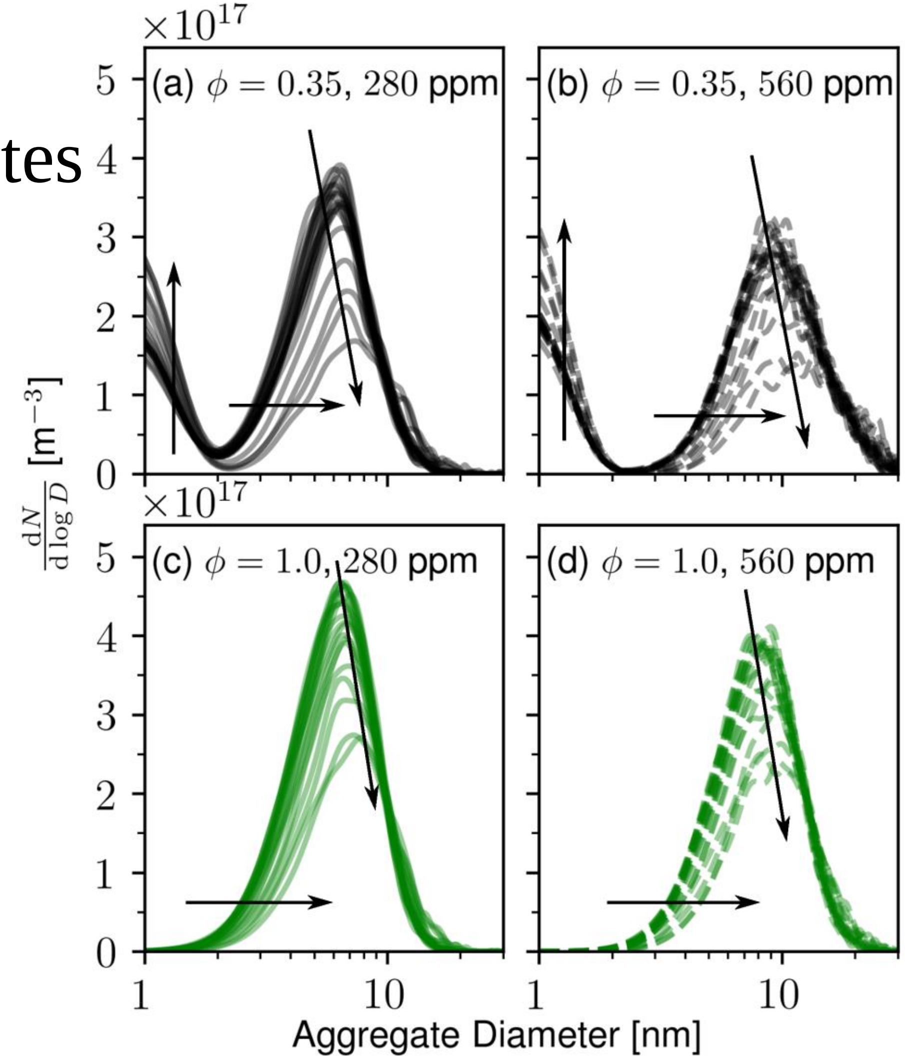

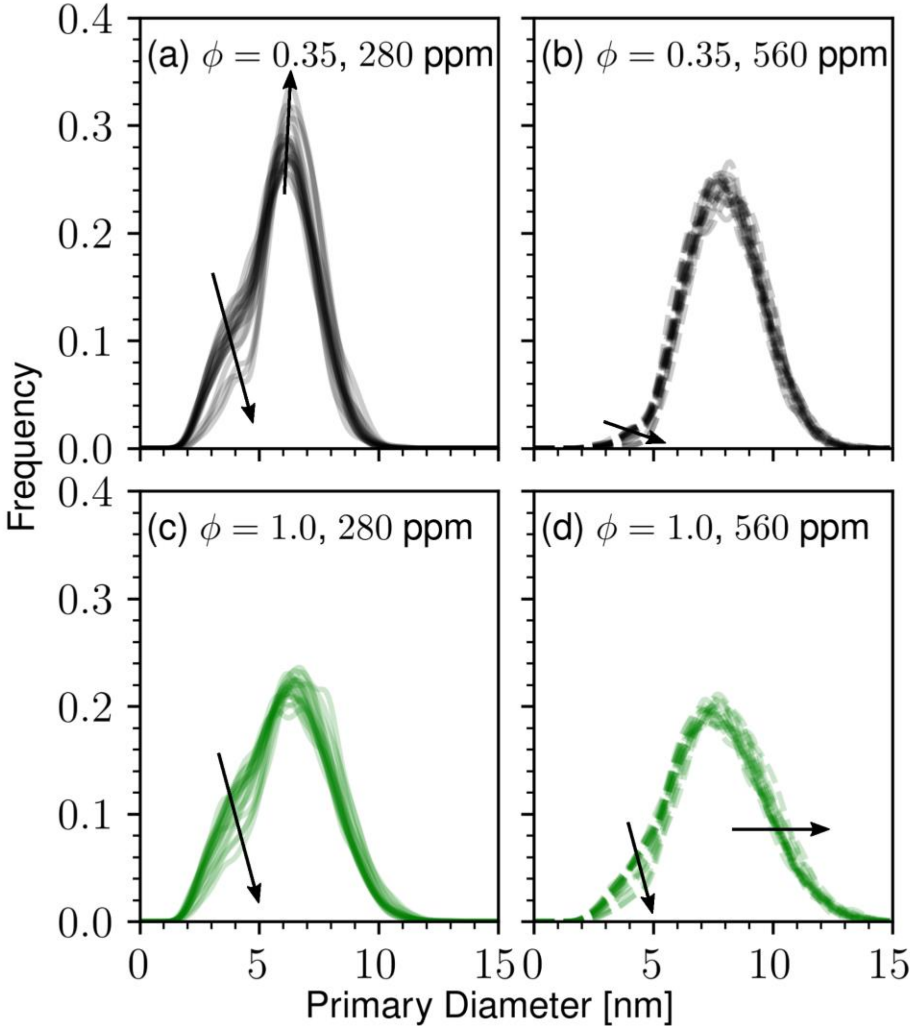

Primaries

Function of deposition radius

Aggregates

Changes to PSD are driven by more coagulation

Primaries

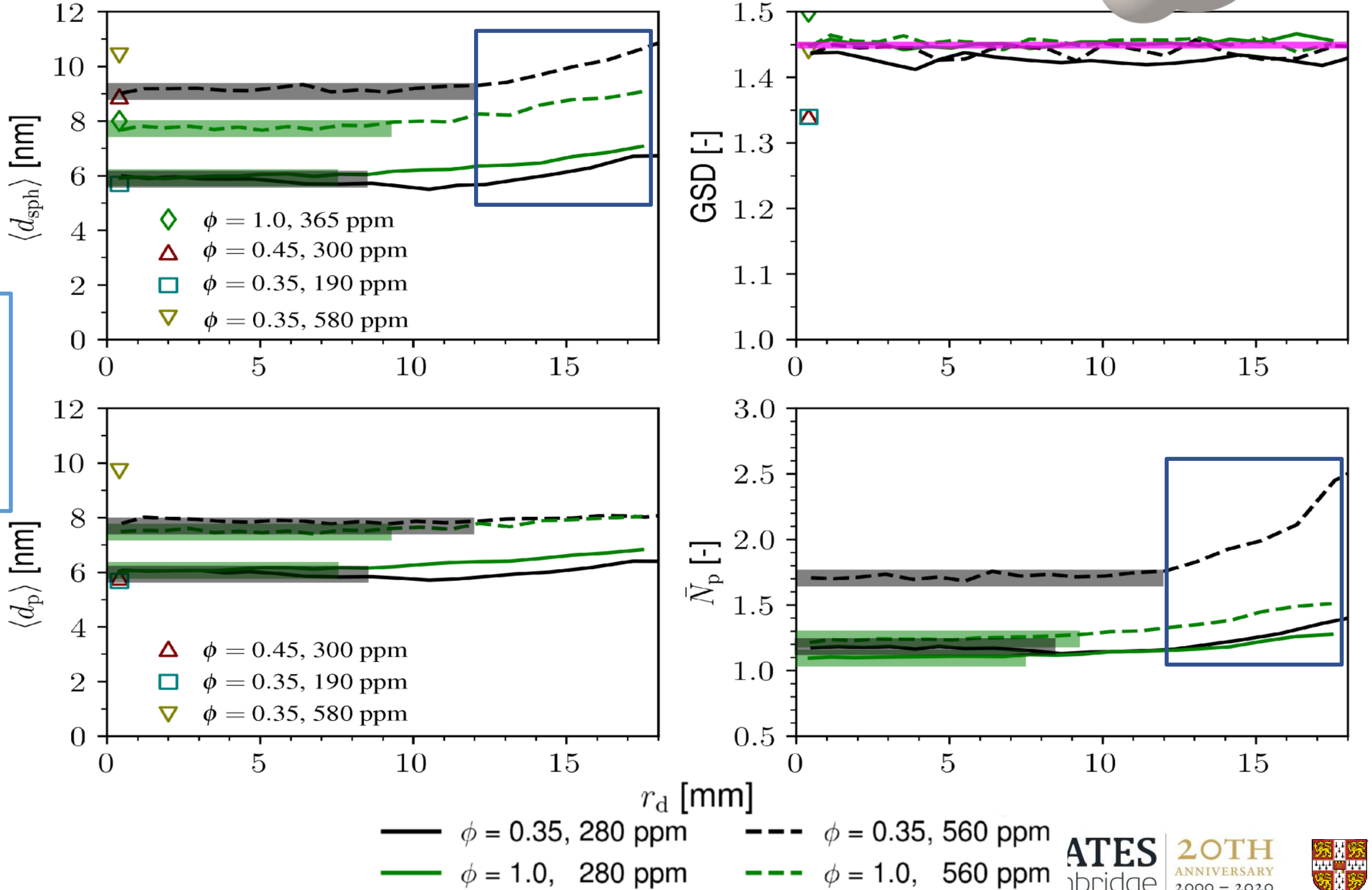

Contributions

Four flames simulated in 2D

Detailed Particle model provided insight into PSD

PSD differed at ≈ 1.5 nozzle radius due to coagulation

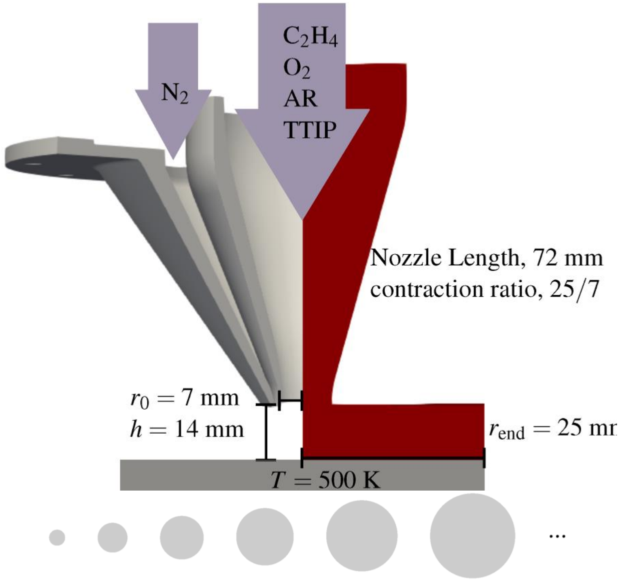

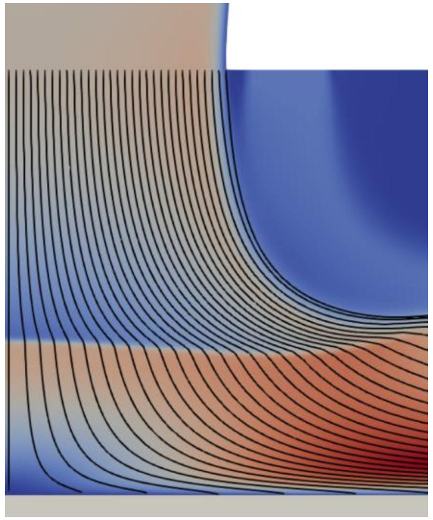

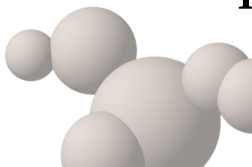

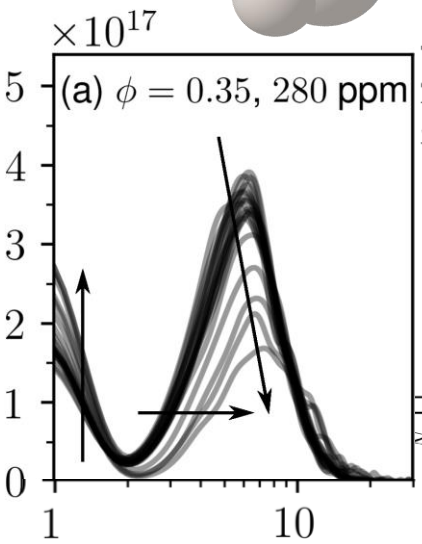

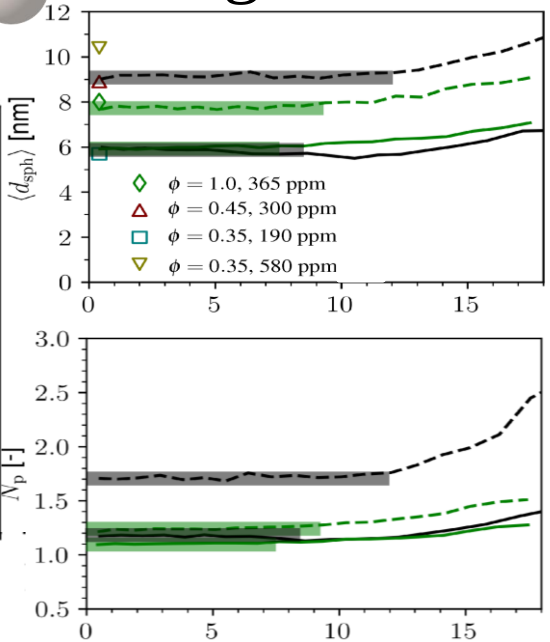

Check performance of synthesized particles is radially uniform

Group

Preprint

CoMo GROUP

CMCL Innovations

GATES Cambridge 20TH ANNIVERSARY 2000 – 2020

Team

Eric Bringley

Manoel Manuputty

Casper Lindberg

Gustavo Leon

Jethro Akroyd

Markus Kraft

CFD Equations

$$\frac{\partial \rho}{\partial t} + \nabla \cdot (\rho U) = 0;$$

$$\frac{\partial \rho U}{\partial t} + \nabla \cdot (\rho U U) = -\nabla p - \mu \left(\nabla U + (\nabla U)^{\mathsf{T}}\right);$$

$$\frac{\partial \rho Y_i}{\partial t} + \nabla \cdot (\rho U Y_i) + \nabla \cdot (\rho V_i^c Y_i) = \dot{\omega}_i;$$

$$c_p \frac{\partial \rho T}{\partial t} + c_p \nabla \cdot (\rho U T) = \nabla \cdot (\lambda \nabla T) - \left(\rho \sum_{i=1}^{N} c_{p_i} Y_i V_i^c \right) \cdot \nabla T + \dot{\omega}_{\mathrm{T}}$$

$$\frac{\partial \rho \hat{M}_j}{\partial t} + \nabla \cdot (\rho U \hat{M}_j) + \nabla \cdot (\rho V_{\mathrm{T}} \hat{M}_j) = \nabla \cdot \left(\rho D_{\mathrm{p}_1} \nabla \hat{M}_{j-\frac{2}{3}} \right) + \dot{\omega}_j$$

Closure Models

Viscosity

$$\mu = \sum_{i=1}^{N} \frac{X_i \mu_i}{\sum_{j=1}^{N} X_j \phi_{ij}}$$

$$\phi_{ij} = \frac{1}{\sqrt{8}} \left(1 + \frac{W_i}{W_j}\right)^{-\frac{1}{2}} \left(1 + \left(\frac{\mu_i}{\mu_j}\right)^{\frac{1}{2}} \left(\frac{W_j}{W_i}\right)^{\frac{1}{4}}\right)^2$$

Thermal Conductivity

$$\lambda = \frac{1}{2} \left(\sum_{i=1}^{N} X_i \lambda_i + \left[\sum_{i=1}^{N} X_i / \lambda_i \right]^{-1} \right)$$

Diffusion

Binary $$D_{i,j} = \frac{3}{16} \left(\frac{2 N_A k_B^3 T^3}{\pi W_{ij}} \right)^{1/2} \frac{1}{p \sigma_{ij}^2 \Omega^{(1,1*)}}$$

Mixture-Averaged: $$D_i = \frac{1 - Y_i}{\sum_{j \neq i}^{N} \frac{X_j}{D_{ij}}}$$

Diffusion Velocity: $$V_i = -D_i \frac{\nabla X_i}{X_i}, \quad V_c = -\sum_{j}^{N} Y_j V_j$$

Corrected Diffusion Velocity: $$V_i^c = V_i + V_c$$

Closure Models

Thermodynamic Properties, JANAF Polynomials

$$c_{p_i} = \frac{C_{p_i}}{W_i} = \frac{\mathrm{R_g}}{W_i}\left(a_{1,i} + a_{2,i}T + a_{3,i}T^2 + a_{4,i}T^3 + a_{5,i}T^4\right) \qquad c_p = \sum_{i=1}^{\mathrm{N_{sp}}} Y_i c_{p_i}$$

$$h_i = \frac{H_i}{W_i} = \frac{\mathrm{R_g}}{W_i}\left(a_{1,i}T + \frac{a_{2,i}}{2}T^2 + \frac{a_{3,i}}{3}T^3 + \frac{a_{4,i}}{4}T^4 + \frac{a_{5,i}}{5}T^5 + a_{6,i}\right) \qquad h = \sum_{i=1}^{\mathrm{N_{sp}}} Y_i h_i$$

Ideal Gas Law

$$pV = nRT$$

Models and methods: flow

2D Simulations:
Navier Stokes Equations,
CFD with PISO Alg.

CFD Models:
Ideal Gas Law, JANAF,
Mixture Avg. Transport,
UCSD Chemistry

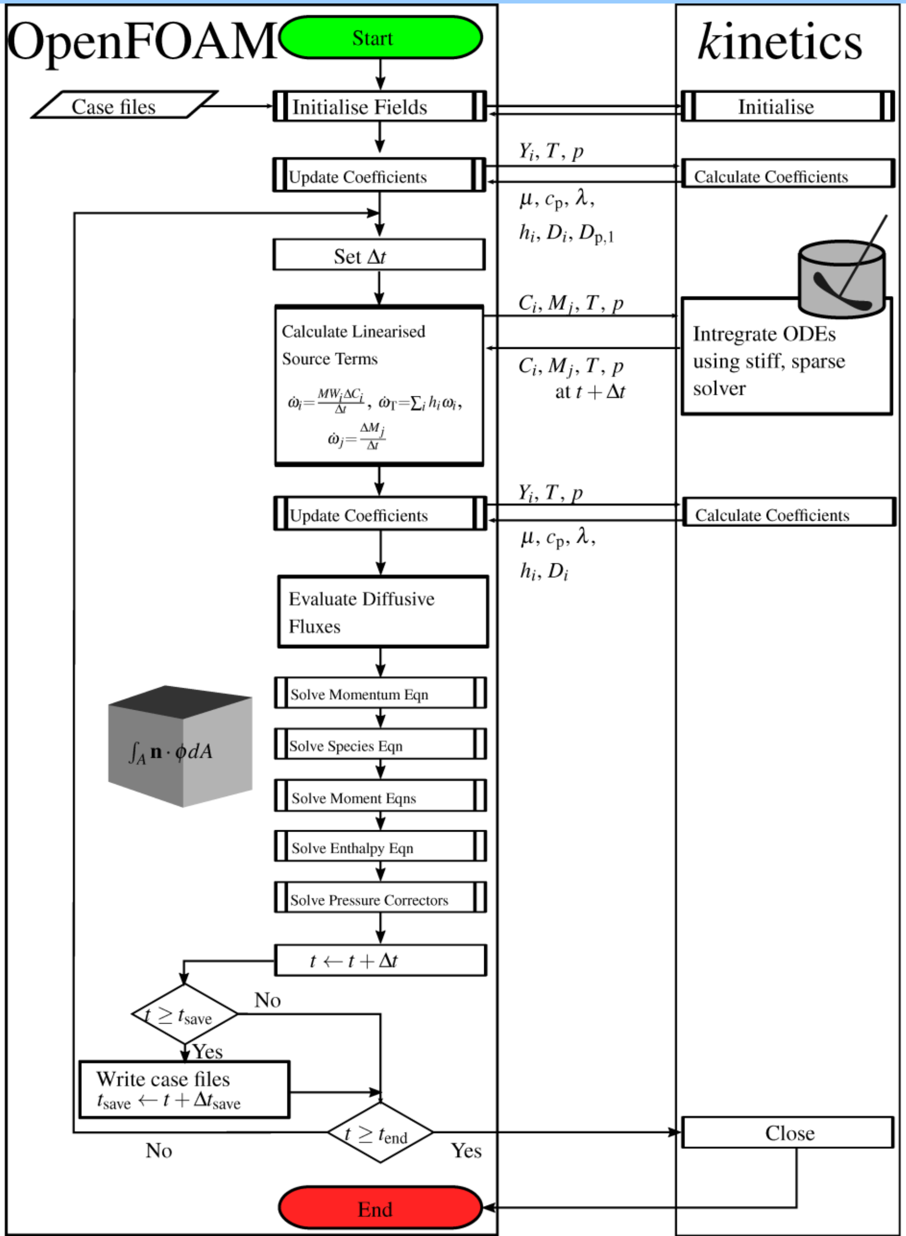

CoMo GROUP
CMCL Innovations

Models and methods: TiO$_2$ particles

Computational efficiency
vs
Physical insight

Same gas phase transfer species, Ti(OH)$_4$
Particle inception, surface growth, and coagulation

Coupled to governing equations

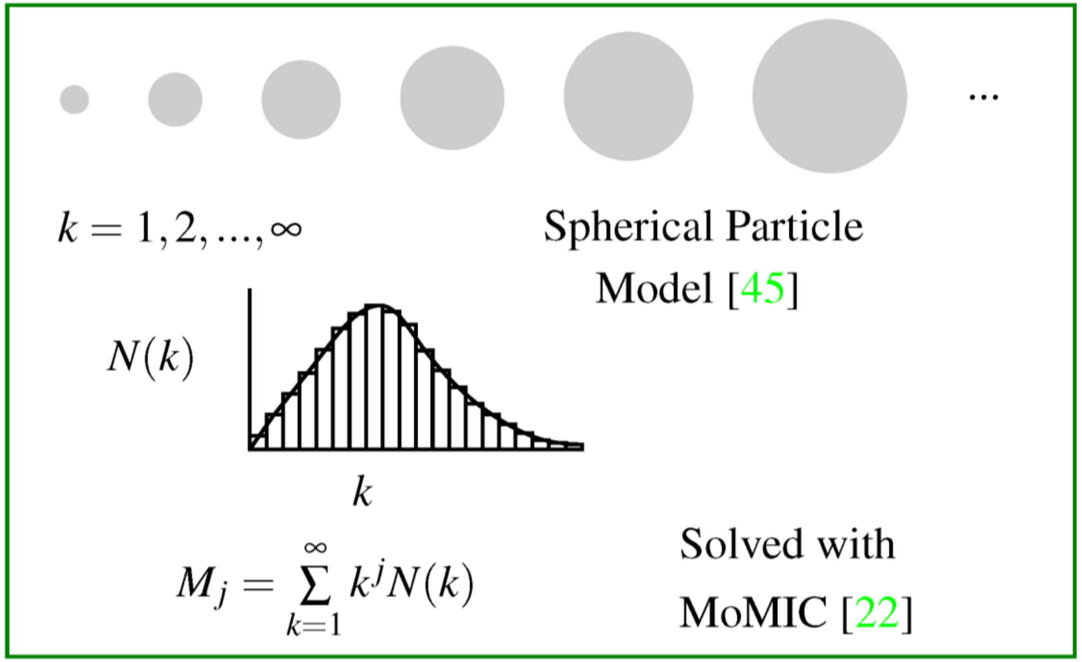

$k = 1, 2, \ldots, \infty$

Spherical Particle Model [45]

$$M_j = \sum_{k=1}^{\infty} k^j N(k)$$

Solved with MoMIC [22]

Lagrangian post-processing

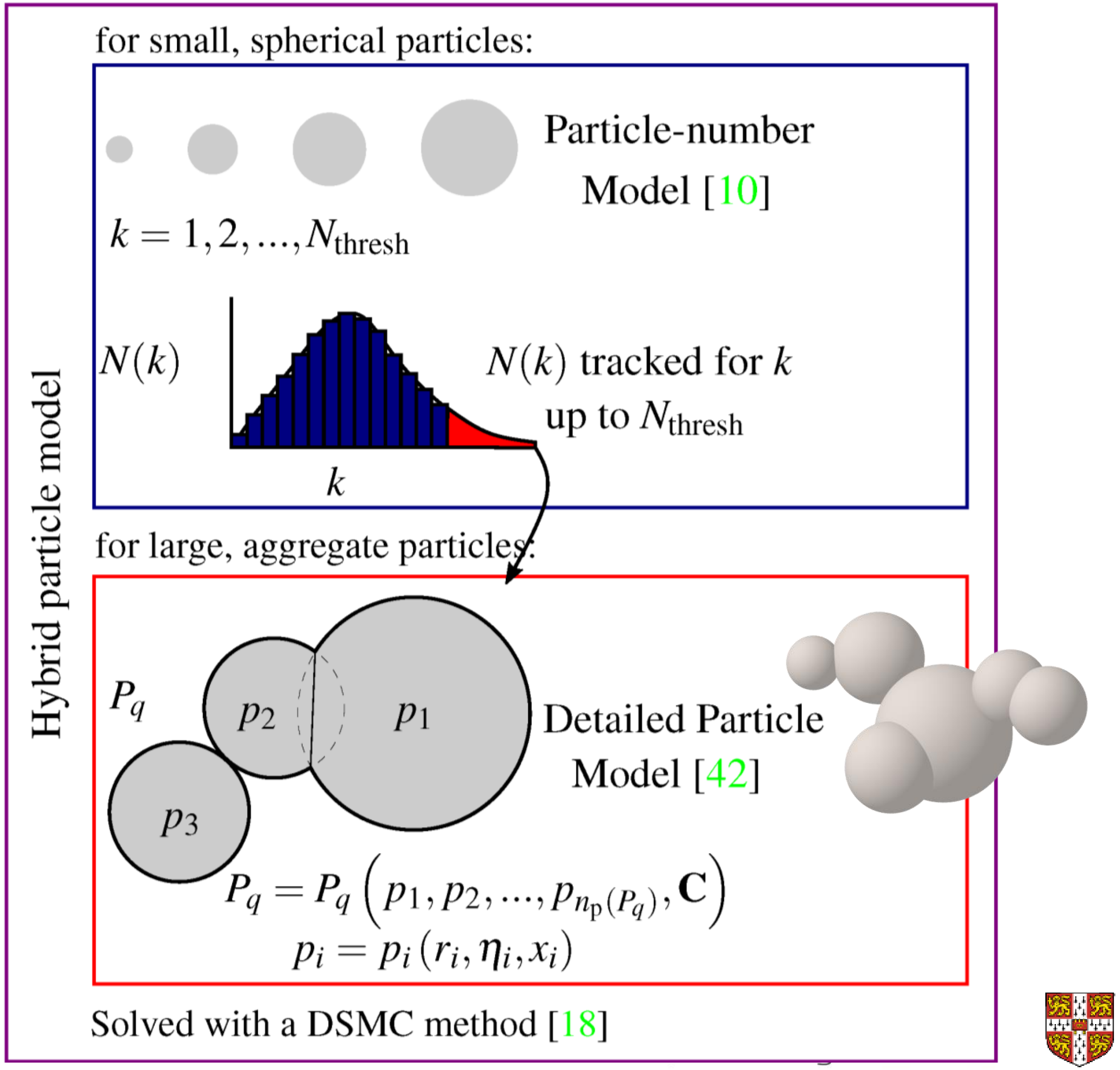

for small, spherical particles:

Particle-number Model [10]

$k = 1, 2, \ldots, N_{\text{thresh}}$

$N(k)$ tracked for k up to N_{thresh}

for large, aggregate particles:

Detailed Particle Model [42]

$$P_q = P_q\left(p_1, p_2, \ldots, p_{n_p(P_q)}, \mathbf{C}\right)$$
$$p_i = p_i\left(r_i, \eta_i, x_i\right)$$

Solved with a DSMC method [18]

Flame data

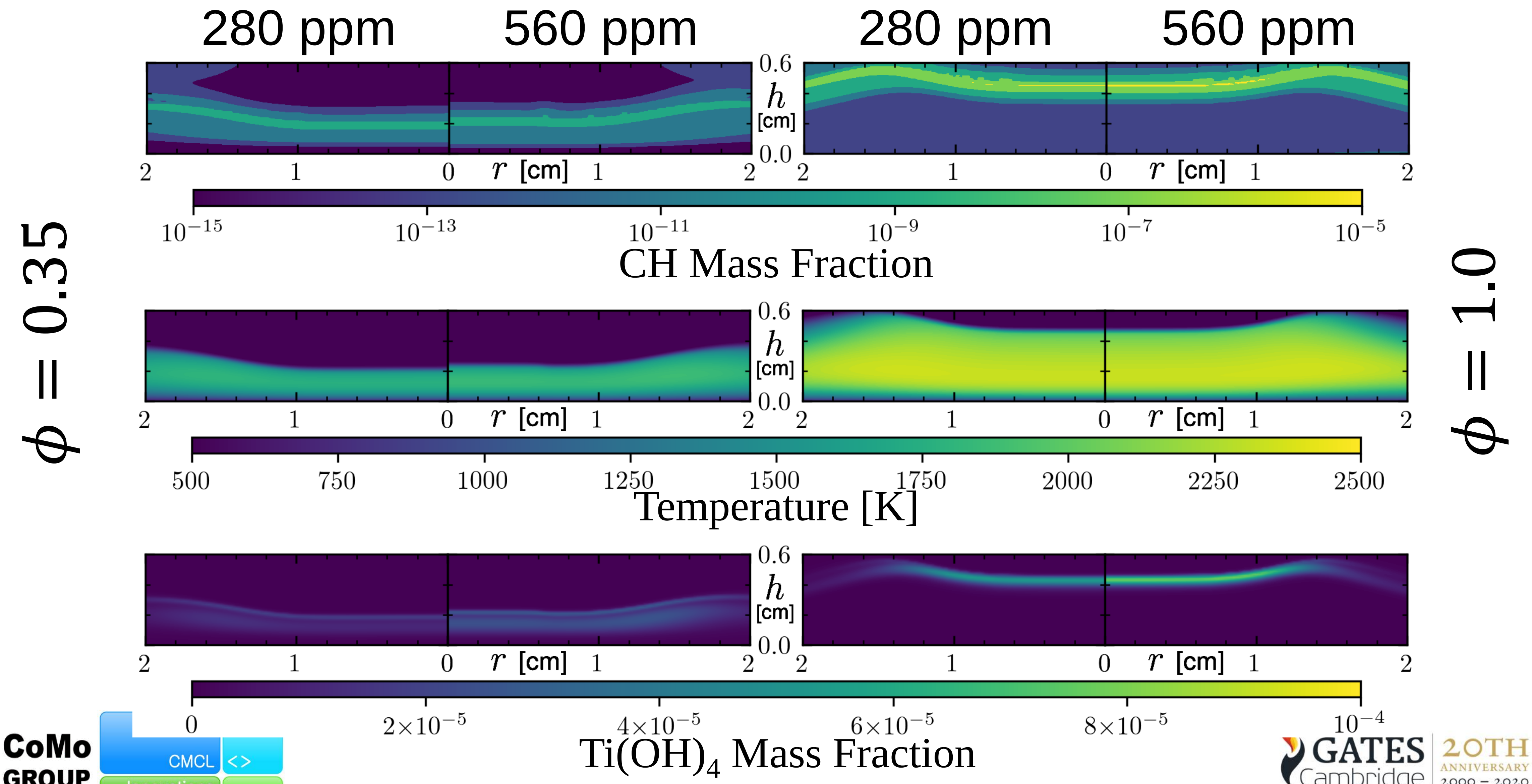
280 ppm
560 ppm
280 ppm
560 ppm
0.6
h
[cm]
0.0
2
1
0
r [cm]
1
2
10^{-15}
10^{-13}
10^{-11}
10^{-9}
10^{-7}
10^{-5}
CH Mass Fraction
$\phi = 0.35$
$\phi = 1.0$
500
750
1000
1250
1500
1750
2000
2250
2500
Temperature [K]
0
2×10^{-5}
4×10^{-5}
6×10^{-5}
8×10^{-5}
10^{-4}
$Ti(OH)_4$ Mass Fraction

Trajectory properties

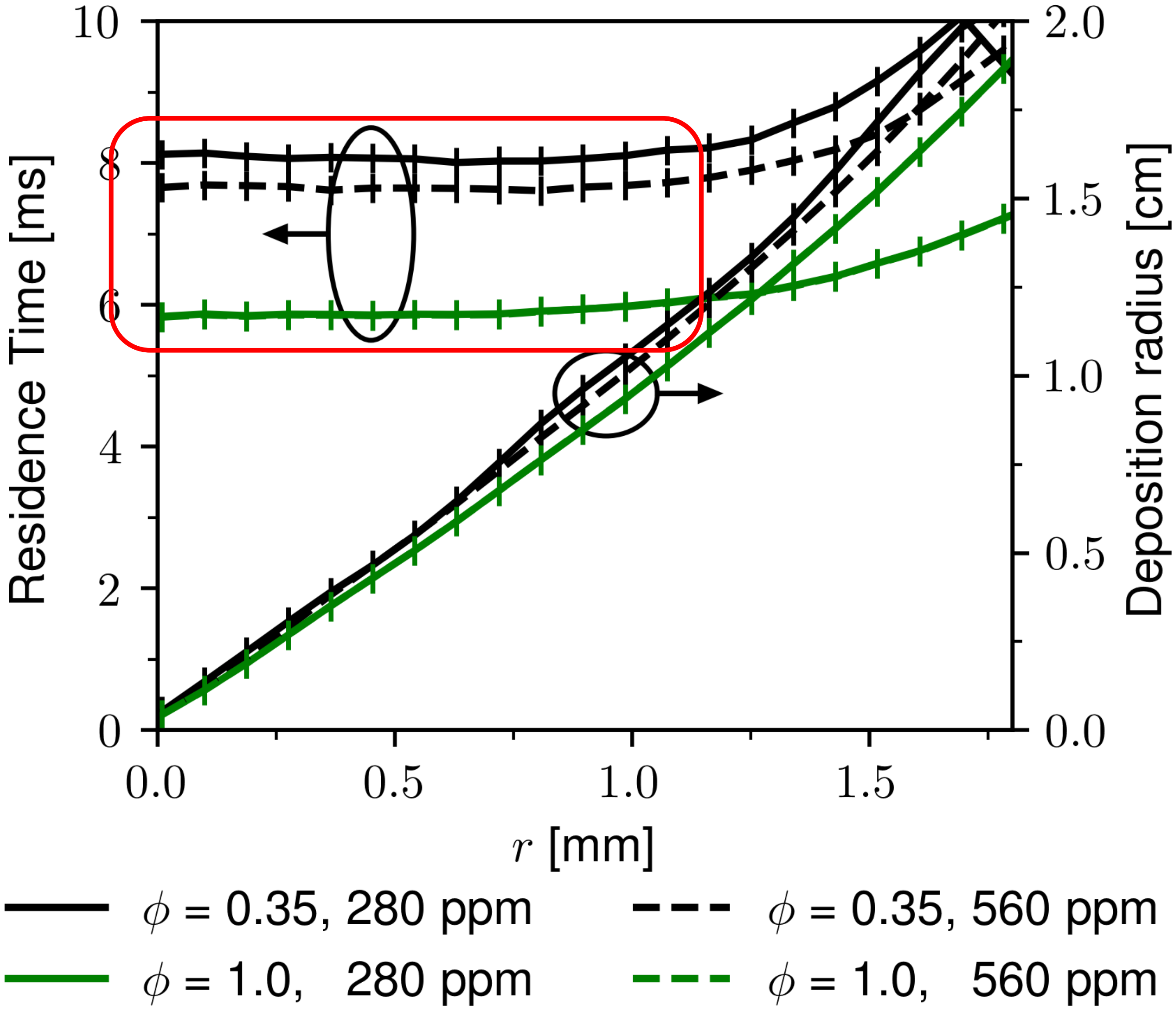

Primaries particle joint property distributions

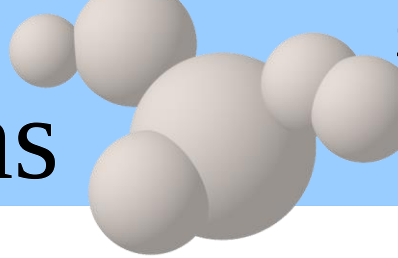

Average primary diameter does not significantly change

Large particles at large radius have a high number of primaries

Large particles are weakly sintered

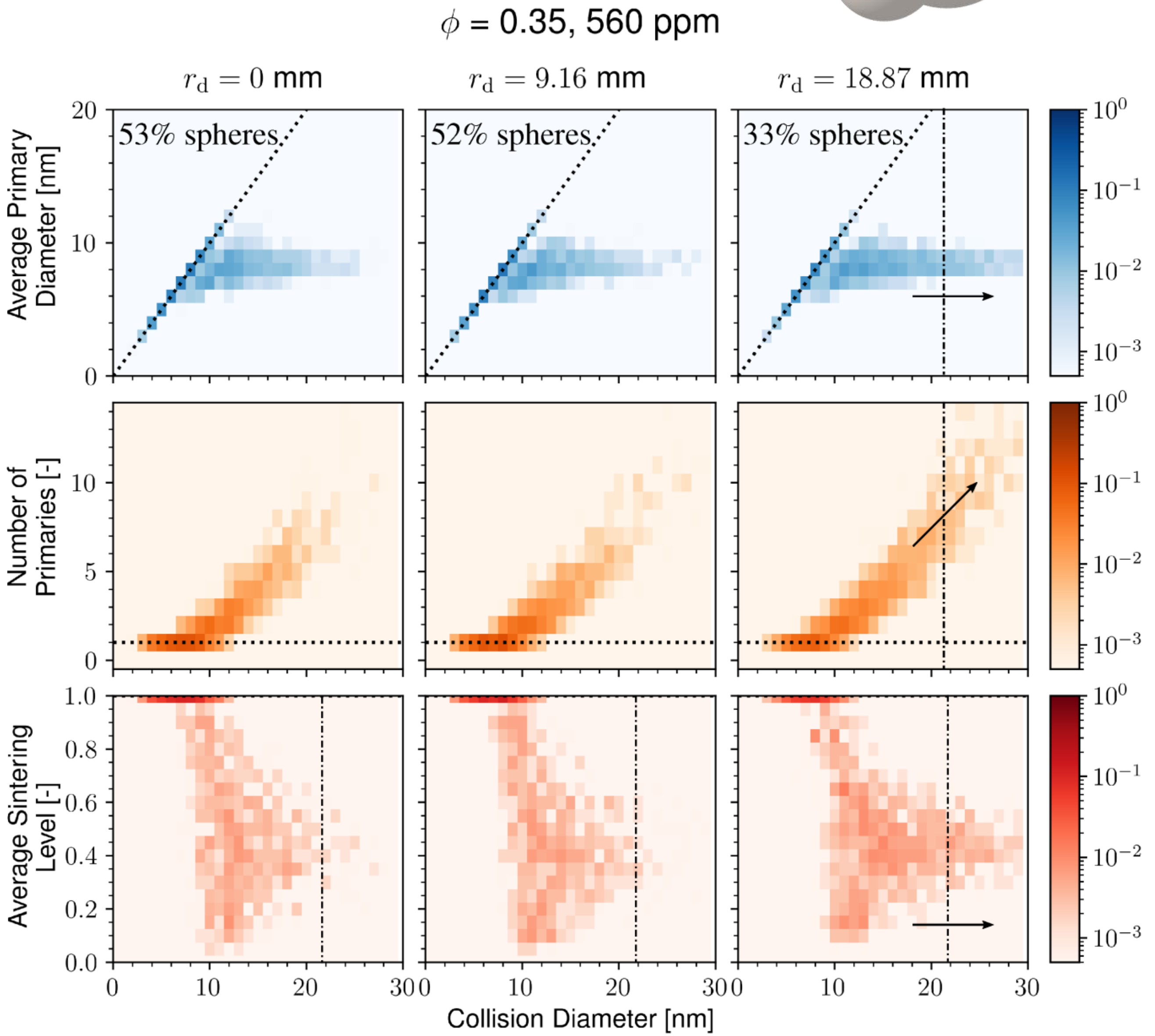

CoMo
GROUP

CMCL
Innovations

Titania crystal phases

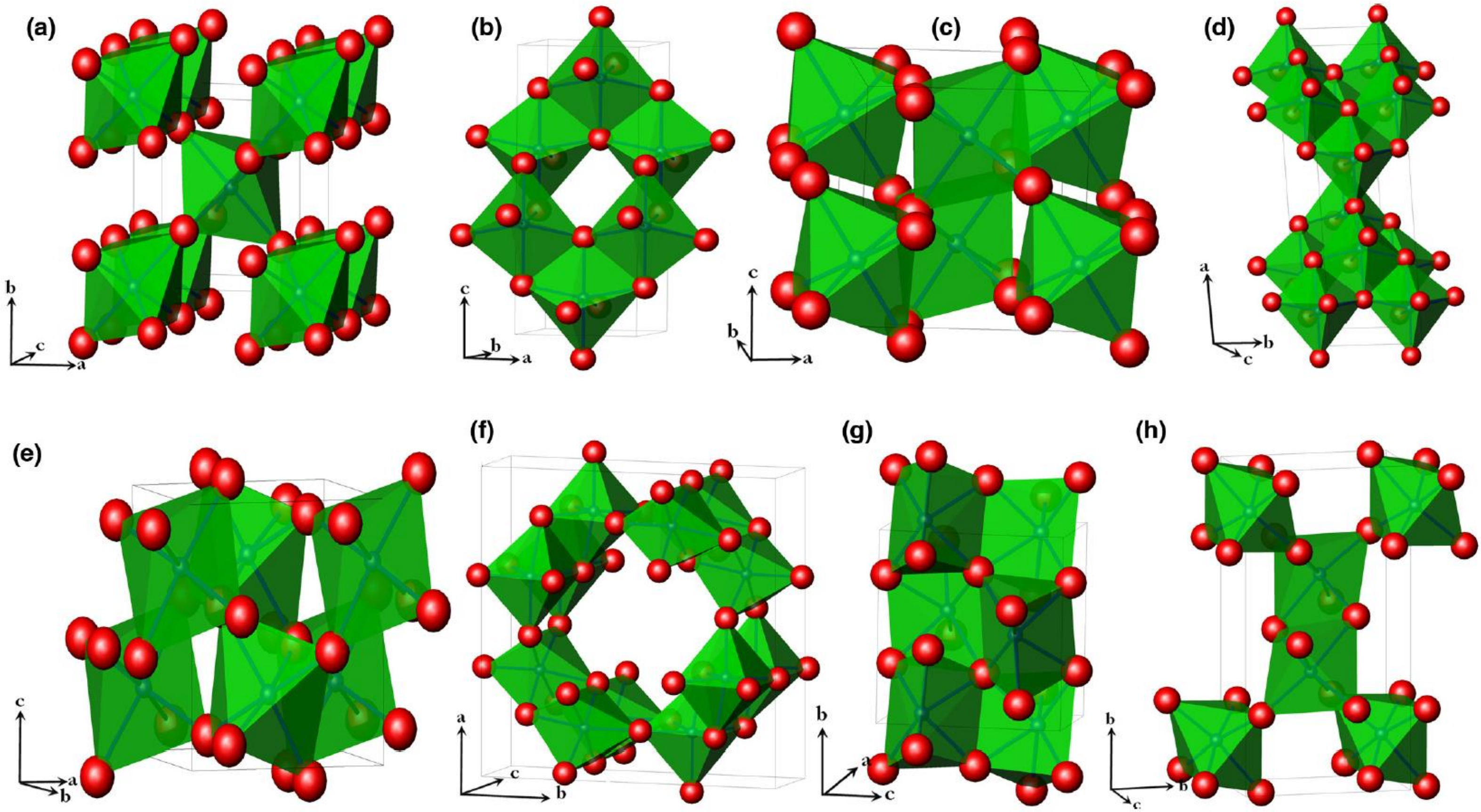

(a) Rutile
(b) Anatase
(c) Bronze
(d) Brookite
(e) Columbite
(f) Hollandite
(g) Baddeleyite
(h) Ramsdellite

Figure from Aravindan et. al (2015), https://doi.org/10.1016/j.mattod.2015.02.015